DRAFT VERSION MAY 19, 2009
Preprint typeset using LaTeX style emulateapj v. 10/09/06

arXiv:0902.0794v2 [astro-ph.HE] 19 May 2009

ON THE SATURATION OF THE MAGNETOROTATIONAL INSTABILITY VIA PARASITIC MODES

MARTIN E. PESSAH
Institute for Advanced Study, Princeton, NJ, 08540

AND

JEREMY GOODMAN
Princeton University Observatory, Princeton, NJ 08544
Draft version May 19, 2009

ABSTRACT

We investigate the stability of incompressible, exact, non-ideal magnetorotational (MRI) modes against parasitic instabilities. Both Kelvin-Helmholtz and tearing-mode parasitic instabilities may occur in the dissipative regimes accessible to current numerical simulations. We suppose that a primary MRI mode saturates at an amplitude such that its fastest parasite has a growth rate comparable to its own. The predicted alpha parameter then depends critically on whether the fastest primary and parasitic modes fit within the computational domain and whether non-axisymmetric parasitic modes are allowed. Hence even simulations that resolve viscous and resistive scales may not saturate properly unless the numerical domain is large enough to allow the free evolution of both MRI and parasitic modes. To minimally satisfy these requirements in simulations with vertical background fields, the vertical extent of the domain should accommodate the fastest growing MRI mode while the radial and azimuthal extents must be twice as large. The fastest parasites have horizontal wavelengths roughly twice as long as the vertical wavelength of the primary.

Subject headings: accretion, accretion disks — black hole physics — instabilities — MHD — turbulence

1. INTRODUCTION

Understanding the processes that halt the exponential growth of the magnetorotational instability (MRI; Velikhov 1959; Chandrasekhar 1960; Balbus & Hawley 1991, 1998) and set the rate of angular momentum transport in the turbulent regime has been an outstanding problem in accretion physics for almost two decades. The net magnetic flux (Hawley et al. 1995; Sano et al. 2004; Pessah et al. 2007), the geometry of the domain (Hawley et al. 1995; Bodo et al. 2008), the resolution (Pessah et al. 2007; Fromang & Papaloizou 2007), and the microphysical dissipation coefficients (Fleming et al. 2000; Sano & Inutsuka 2001; Fromang et al. 2007; Lesur & Longaretti 2007; Masada & Sano 2008), all influence the non-linear saturation of the MRI in simulations.

Saturation of the MRI may be related to secondary (parasitic) instabilities (Goodman & Xu 1994, hereafter GX94) that feed upon the free energy afforded by the MRI (see, e.g., Knobloch & Julien 2005; Umurhan et al. 2007; Tatsuno & Dorland 2008; Vishniac 2009 for alternative ideas). These instabilities are often invoked to explain some of the behavior observed in numerical simulations. The absence of explicit dissipation from most numerical studies and from GX94's analysis, however, impedes quantitative interpretations.

Both primary and secondary instabilities may be subject to non-ideal effects. The growth rates and wavenumbers of the fastest growing MRI primaries, and the relative orientations and magnitudes of their velocity and magnetic field perturbations, are sensitive to dissipation coefficients (see, e.g., Lesur & Longaretti 2007; Lesaffre & Balbus 2007; Pessah & Chan 2008). Viscosity may slow the growth of the Kelvin-Helmholtz secondaries identified by GX94, and non-zero resistivity may enable resistive instabilities such as tearing modes (see, e.g., Boyd & Sanderson 2003).

Electronic address: mpessah@ias.edu, jeremy@astro.princeton.edu

Here we summarize a parametric study of parasitic instabilities in dissipative regimes accessible to current numerical simulations. We adopt the incompressible limit, which is relevant for initial fields so weak that saturation occurs with sub-equipartition fields. The fastest growing, non-ideal parasitic modes are related to Kelvin-Helmholtz and tearing-mode instabilities. They are non-axisymmetric and have horizontal wavelengths roughly a factor of 2 larger than the vertical wavelength of the primary MRI mode. Our findings suggest that current simulation domains may bias the saturation of the non-ideal MRI by excluding the fastest MRI and parasitic modes (see also Hawley et al. 1995; Sano 2007; Bodo et al. 2008).

2. VISCOUS, RESISTIVE PRIMARY MRI MODES

Consider an incompressible, Keplerian background with constant viscosity ν and resistivity η and threaded by a vertical magnetic field, $\bar{B}_z$, against perturbations parallel to the background magnetic field. Pessah & Chan (2008) showed that in the shearing box, exact unstable solutions exist of the form

$$\boldsymbol{v} = -q\Omega_0(r-r_0)\hat{\boldsymbol{\phi}} + \boldsymbol{V}_0 \sin(Kz)\, e^{\Gamma t}\,, \tag{1}$$

$$\boldsymbol{B} = \bar{B}_z\hat{\boldsymbol{z}} + \boldsymbol{B}_0 \cos(Kz)\, e^{\Gamma t}\,, \tag{2}$$

where $q \equiv -d\ln\Omega/d\ln r$ and Ω_0 is the local Keplerian frequency. For a given wavenumber K, the growth rate Γ satisfies the dispersion relation

$$(K^2\bar{v}_{\mathrm{A}z}^2+\Gamma_\nu\Gamma_\eta)^2+\kappa^2(K^2\bar{v}_{\mathrm{A}z}^2+\Gamma_\eta^2)-4K^2\bar{v}_{\mathrm{A}z}^2\Omega_0^2 = 0\,, \tag{3}$$

where $\Gamma_\nu \equiv \Gamma + \nu K^2$, $\Gamma_\eta \equiv \Gamma + \eta K^2$, $\kappa \equiv \sqrt{2(2-q)}\Omega_0$ is the epicyclic frequency, $\bar{v}_{\mathrm{A}z} \equiv \bar{B}_z/\sqrt{4\pi\rho}$ is the Alfvén speed, and ρ is the density. The relative strength

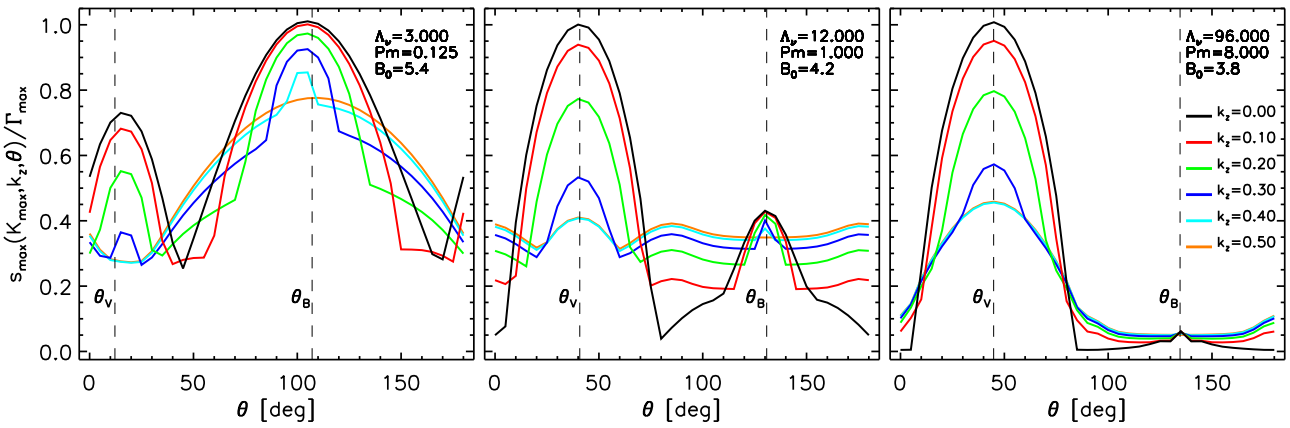

FIG. 1.— Normalized growth rates of the fastest growing parasitic modes vs. the orientation of the horizontal wavevector $\boldsymbol{k}_{\rm h}$ with respect to the radial ($\theta = 0$) direction. In each panel, the MRI magnetic field $B_0 = B_0^{\rm sat}(\nu,\eta)$ is such that the fastest parasitic growth rate, maximized over $k_{\rm h}$, θ and k_z, matches the growth rate of the fastest primary MRI mode, $\Gamma_{\rm max}(\nu,\eta)$, for the indicated "viscous Elsasser" and magnetic Prandtl numbers, Λ_ν and ${\rm Pm}$. The angles $\theta_{\rm V}$ and $\theta_{\rm B}$ mark the directions of the horizontal velocity and magnetic fields of the fastest MRI mode. The fastest parasites lie at $\theta \approx \theta_{\rm V}$ or $\theta \approx \theta_{\rm B}$ and are associated with Kelvin-Helmholtz and tearing mode instabilities, respectively. Tearing modes gain prominence at lower ${\rm Pm}$.

V_0/B_0 of the MRI velocity and magnetic fields, $\boldsymbol{V}_0 = V_0\,(\cos\theta_{\rm V}, \sin\theta_{\rm V}, 0)$ and $\boldsymbol{B}_0 = B_0\,(\cos\theta_{\rm B}, \sin\theta_{\rm B}, 0)$, and their directions $\theta_{\rm V}$ and $\theta_{\rm B}$, are known functions of (ν,η,K). The growth rate Γ has a unique maximum, $\Gamma_{\rm max}(\nu,\eta)$, at $K = K_{\rm max}(\nu,\eta)$.

Numerical simulations impose periodicity lengths on the shearing box. We avoid finite-volume effects in our analysis by adopting length and time scales based on intensive parameters: $L_0 \equiv \bar{v}_{{\rm A}z}/\Omega_0$ and $T_0 \equiv 1/\Omega_0$. Viscosity and resistivity introduce two new scales, which we subsume into the dimensionless quantities $\Lambda_\nu \equiv \bar{v}_{{\rm A}z}^2/\nu\Omega_0$ and $\Lambda_\eta \equiv \bar{v}_{{\rm A}z}^2/\eta\Omega_0$, whose ratio is the magnetic Prandtl number, ${\rm Pm} \equiv \Lambda_\eta/\Lambda_\nu = \nu/\eta$. The quantity Λ_η is known as the Elsasser number, while its viscous counterpart Λ_ν is related to the Reynolds number (see below). Throughout the rest of the Letter, unless otherwise mentioned, we use the scales L_0 and T_0 to define dimensionless variables. In these units, magnetic field strengths are defined relative to the background field $\bar{B}_z$, while $\Lambda_\nu \to \nu^{-1}$ and $\Lambda_\eta \to \eta^{-1}$.

3. VISCOUS, RESISTIVE PARASITIC MODES

To facilitate our analysis of the stability of the non-ideal MRI modes against parasitic instabilities, we invoke some approximations similar to those adopted by GX94 for ideal magnetohydrodynamics (MHD). We assume that the amplitudes of the primary modes are large enough that we can neglect the influence of the weak vertical background field, the Coriolis force, and the background shear flow on the dynamics of the secondary modes. Furthermore, the energy source for secondary instabilities should increase with (some power of) the amplitudes of the primary modes. Therefore, the secondary growth rates should eventually outstrip the primary ones. We thus assume, following GX94, that we can neglect the temporal variation of the sinusoidal velocity and magnetic fields of the primary modes.

Under these assumptions, the equations governing the dynamics of the secondary instabilities are

$$\partial_t \delta\boldsymbol{v} + (\Delta\boldsymbol{v}\cdot\boldsymbol{\nabla})\,\delta\boldsymbol{v} + (\delta\boldsymbol{v}\cdot\boldsymbol{\nabla})\,\Delta\boldsymbol{v} = -\boldsymbol{\nabla}(\delta P + \Delta\boldsymbol{B}\cdot\delta\boldsymbol{B}) + (\Delta\boldsymbol{B}\cdot\boldsymbol{\nabla})\delta\boldsymbol{B} + (\delta\boldsymbol{B}\cdot\boldsymbol{\nabla})\Delta\boldsymbol{B} + \nu\boldsymbol{\nabla}^2\delta\boldsymbol{v}\,, \quad (4)$$

$$\partial_t \delta\boldsymbol{B} + (\Delta\boldsymbol{v}\cdot\boldsymbol{\nabla})\,\delta\boldsymbol{B} + (\delta\boldsymbol{v}\cdot\boldsymbol{\nabla})\,\Delta\boldsymbol{B} = (\Delta\boldsymbol{B}\cdot\boldsymbol{\nabla})\,\delta\boldsymbol{v} + (\delta\boldsymbol{B}\cdot\boldsymbol{\nabla})\,\Delta\boldsymbol{v} + \eta\boldsymbol{\nabla}^2\delta\boldsymbol{B}\,, \quad (5)$$

where $\Delta\boldsymbol{v} \equiv \boldsymbol{V}_0\sin(Kz)$, $\Delta\boldsymbol{B} \equiv \boldsymbol{B}_0\cos(Kz)$, $\boldsymbol{\nabla}\cdot\delta\boldsymbol{v} = \boldsymbol{\nabla}\cdot\delta\boldsymbol{B} = 0$, and δP stands for the pressure perturbation. We seek solutions of the form

$$\delta\boldsymbol{v}(\boldsymbol{x},t) = \delta\boldsymbol{v}_0(z)\,\exp\left[st - i\boldsymbol{k}\cdot\boldsymbol{x}\right], \quad (6)$$

$$\delta\boldsymbol{B}(\boldsymbol{x},t) = \delta\boldsymbol{B}_0(z)\,\exp\left[st - i\boldsymbol{k}\cdot\boldsymbol{x}\right], \quad (7)$$

where the amplitudes $\delta\boldsymbol{v}_0(z)$ and $\delta\boldsymbol{B}_0(z)$ are periodic in z with period $2\pi/K$. Substituting expressions (6) and (7) into Equations (4) and (5), and using the divergenceless nature of the perturbed fields, we derive a set of higher order differential equations for the vertical components of the secondary velocity and magnetic fields,

$$(s+\nu\mathcal{Q})\mathcal{Q}\delta v_z - i(\boldsymbol{k}_{\rm h}\cdot\Delta\boldsymbol{v})(\mathcal{Q}-K^2)\delta v_z + i(\boldsymbol{k}_{\rm h}\cdot\Delta\boldsymbol{B})(\mathcal{Q}-K^2)\delta B_z = 0\,, \quad (8)$$

$$(s+\eta\mathcal{Q})\delta B_z + i(\boldsymbol{k}_{\rm h}\cdot\Delta\boldsymbol{B})\delta v_z - i(\boldsymbol{k}_{\rm h}\cdot\Delta\boldsymbol{v})\delta B_z = 0\,, \quad (9)$$

where the horizontal wavevector $\boldsymbol{k}_{\rm h}$ is such that $\boldsymbol{k} = \boldsymbol{k}_{\rm h} + k_z\hat{\boldsymbol{z}}$, and the differential operator $\mathcal{Q} \equiv k_{\rm h}^2 - \partial_z^2$. The ratio k_z/K need not be rational but $0 \le k_z/K \le 1/2$ (GX94). Equations (8) and (9), with suitable boundary conditions, pose an eigenvalue problem[1] for the parasitic growth rate $s = s(\nu,\eta,K,B_0,k_z,\theta,k_{\rm h})$, where θ denotes the angle between the horizontal wavevector $\boldsymbol{k}_h$ and the radial direction.

Lesur & Longaretti (2007, hereafter LL07) carried out a systematic study of the saturation of the MRI in incompressible MHD with explicit viscosity and resistivity. They presented results for the dimensionless stress at saturation for a grid of models with ${\rm Pm} = \{0.125, 0.25, 1.0, 4.0, 8.0\}$ and ${\rm Re} \equiv SL_z^2/\nu = \{200, 400, 800, 1600, 3200, 6400\}$, with $S = 3\Omega_0/2$. To relate our results to those of LL07, we translate their Reynolds number Re into $\Lambda_\nu = 3{\rm Re}/2\beta$. Their parameter $\beta \equiv S^2L_z^2/\bar{v}_{{\rm A}z}^2$ is a proxy for the plasma β parameter in a stratified disk with equivalent height L_z (in our units $L_z = 2\sqrt{\beta}/3$). Setting $\beta = 100$, as in LL07, it follows that the values for Re cited above correspond to $\Lambda_\nu = \{3, 6, 12, 24, 48, 96\}$. Note that these are rather small.

We solved equations (8) and (9) for all the possible combinations of the set of values of Λ_ν and ${\rm Pm}$ defined above and searched the parameter space defined by $(B_0, k_z, \theta, k_{\rm h})$ in order to identify the most relevant, fastest growing secondary

[1] The method of solution of these differential equations as well as a discussion of the physics of the secondary modes will be presented elsewhere.

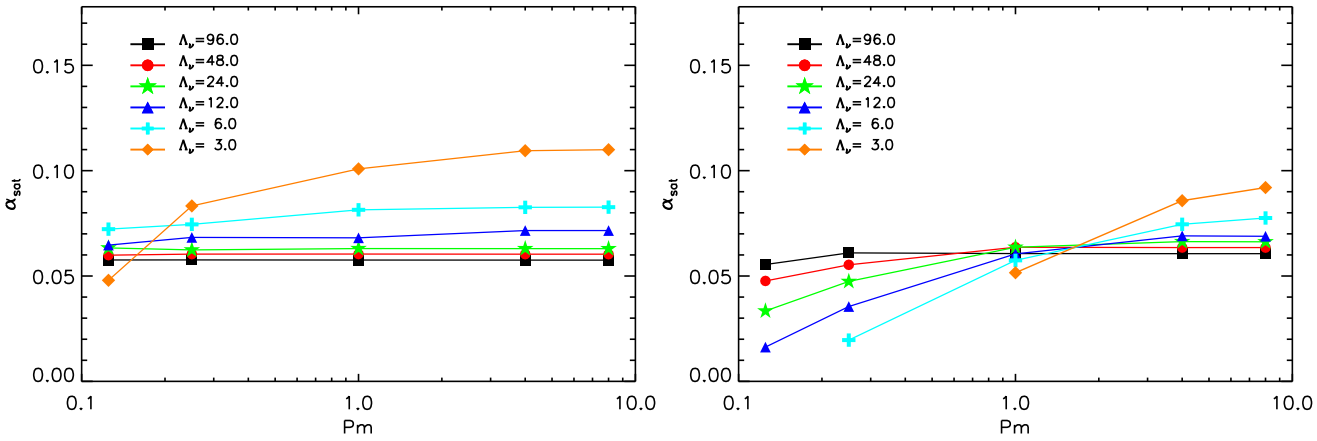

FIG. 2.— Predicted dimensionless stress at saturation, $\alpha_{\rm sat}$, as a function of Λ_ν and Pm, if saturation occurs when the fastest parasitic and primary MRI growth rates match. The indicated values for Λ_ν correspond to the Reynolds numbers studied by LL07, $\mathrm{Re} = \{200, 400, 800, 1600, 3200, 6400\}$. In the left panel the fastest MRI and parasitic modes are allowed to evolve unimpeded. In the right panel the primary and secondary modes considered are the fastest MRI and parasitic modes that can fit in a domain with $(L_r, L_\phi, L_z) = (1, 4, 1) \times 2\sqrt{\beta}/3$ with $\beta = 100$, as considered in LL07.

modes. We have not been able to find unstable parasitic modes with $k_{\rm h} > K$. This result generalizes the findings of GX94 to the non-ideal MHD regime.

4. SATURATION OF THE MAGNETOROTATIONAL INSTABILITY

The secondary modes will be clearly dynamically important when their growth rates are comparable to, or greater than, the growth rates of the primary modes upon which they feed. We refer to this instance as the "saturation" of the primary MRI mode. It is then convenient to define the saturation amplitude $B_0^{\rm sat}(\nu, \eta, K)$ as the amplitude that the magnetic field produced by the MRI must have grown to in order for the instantaneous growth rate of the fastest parasitic mode, $s_{\rm max}(\nu, \eta, K)$, to match that of the primary, $\Gamma(\nu, \eta, K)$[2].

In the ideal limit, the growth rate of the secondary modes derived from equations (8) and (9) is linear in the amplitude of the primary magnetic field (GX94). Thus, the amplitude B_0 at which the growth rate of the fastest secondary equals the growth rate of a given primary mode can be estimated after solving these equations with $\nu = \eta = 0$. However, in the non-ideal case the amplitude B_0 cannot be scaled out of the problem, and the growth rate of the secondary modes depends on it in a non-trivial way. Figure 1 shows the fastest growth rates $s_{\rm max}(\nu, \eta, K_{\rm max}, k_z, \theta)$ of various secondary modes that feed off the fastest primary MRI mode for three combinations of Λ_ν and Pm, with curves for several values of k_z. In all of the cases shown, $B_0 = B_0^{\rm sat}(\nu, \eta, K_{\rm max})$, i.e., the amplitude of the primary MRI mode is such that the fastest secondary growth rate, $s_{\rm max}(\nu, \eta, K_{\rm max}) = \Gamma_{\rm max}(\nu, \eta)$.

For all the cases within the explored dissipative regime, the fastest parasitic modes are non-axisymmetric ($\theta \neq 0$), have the same vertical periodicity as the primary mode ($k_z = 0$), and have purely real growth rates. The fastest modes have horizontal wavevectors that are nearly aligned with either the velocity or the magnetic field of the primary ($\Delta\boldsymbol{v}$, $\Delta\boldsymbol{B}$). The first type are clearly related to Kelvin-Helmholtz instabilities while the latter are related to tearing modes. The ratio between the horizontal wavenumber of the fastest parasitic mode, $k_{\rm h,max}(\nu, \eta, K_{\rm max})$, and the wavenumber of the fastest MRI mode is rather insensitive to either Λ_ν or Pm; $k_{\rm h,max}/K_{\rm max}$ varies from 0.59, in ideal MHD, to 0.46, in the cases with highest viscosity and resistivity.

We calculate the dimensionless stress at saturation as $\alpha_{\rm sat} \equiv \bar{T}_{r\phi}^{\rm sat}/(SL_z)^2$, where $\bar{T}_{r\phi}^{\rm sat} \equiv \bar{R}_{r\phi}^{\rm sat} - \bar{M}_{r\phi}^{\rm sat}$, is the sum of the Reynolds and Maxwell stresses

$$\bar{R}_{r\phi}^{\rm sat} \equiv \frac{1}{L_z}\int_{-L_z/2}^{L_z/2} V_{0,r}^{\rm sat}(z) V_{0,\phi}^{\rm sat}(z) dz\,, \qquad (10)$$

$$\bar{M}_{r\phi}^{\rm sat} \equiv \frac{1}{L_z}\int_{-L_z/2}^{L_z/2} B_{0,r}^{\rm sat}(z) B_{0,\phi}^{\rm sat}(z) dz\,. \qquad (11)$$

These expressions are integrated to obtain the dimensionless stress $\alpha_{\rm sat}$ in terms of the parameter β,

$$\alpha_{\rm sat} = \frac{1}{4\beta}[(V_0^{\rm sat})^2 \sin 2\theta_{\rm V} - (B_0^{\rm sat})^2 \sin 2\theta_{\rm B}]\,. \qquad (12)$$

The left panel of Figure 2 shows $\alpha_{\rm sat}$ in the case where both primary and secondary instabilities evolve unimpeded. There are competitive effects that set the value of $\alpha_{\rm sat}$, which is dominated by the Maxwell stress. As dissipation increases, the saturation amplitude $B_0^{\rm sat}$ increases from $B_0^{\rm sat} = 3.8$, in ideal MHD, to $B_0^{\rm sat} \simeq 5.5$, in the cases with high dissipation. However, the angle $\theta_{\rm B}$ decreases toward $\pi/2$, so that $|\sin 2\theta_{\rm B}|$ decreases. Both effects roughly compensate each other so that the final value of $\alpha_{\rm sat}$ changes only by a factor of 2. Therefore, for the range of dissipation coefficients that we explored, the saturation amplitude of the primary modes should be insensitive to the dissipation coefficients if both the fastest primary and secondary instabilities are permitted. The value of $\alpha_{\rm sat}$ does not depend on Pm for large Λ_ν, and the range of Pm for which the results do not depend on Pm seems to increase with Λ_ν.

The right panel of Figure 2 shows $\alpha_{\rm sat}$ when the primary and secondary modes considered are the fastest MRI and parasitic modes that can fit in a domain $(L_r, L_\phi, L_z) = (1, 4, 1) \times 2\sqrt{\beta}/3$ with $\beta = 100$, as considered in LL07. The purpose of this exercise is to emulate the situation in which a finite simulation domain might constrain the availability of primary and/or secondary modes. The dependence of $\alpha_{\rm sat}$ on the dimensionless numbers $(\Lambda_\nu, \mathrm{Pm})$ is modified with respect to the case where there are no limitations on the range of primary or secondary modes; $\alpha_{\rm sat}$ decreases with decreasing Pm

[2] In neglecting the temporal dependence of the background, it is assumed that the secondary growth rates are large compared to the primary growth rate; thus our definition of saturation implies an extrapolation to the regime where this assumption is not strictly satisfied.

for a wider range of Λ_ν. This trend is similar to that observed by LL07, but the dependence on Pm is less pronounced and the predicted value of $\alpha_{\rm sat}$ is smaller than that found in non-linear simulations (by a factor of 6 at $\mathrm{Pm} = 1$). Most of the differences in $\alpha_{\rm sat}$ associated with domain size are due to the limitations on the primaries. Although the fastest secondaries do not fit in the domain, there are other secondary modes with comparable growth rates that can lead to "saturation" at slightly larger primary amplitudes.

5. DISCUSSION

We have investigated the spectrum of parasitic instabilities that feed off the MRI in viscous, resistive MHD, focusing our attention on the parameter space currently accessible to numerical simulations. Our study suggests that important differences between two-dimensional and three-dimensional simulations are to be expected. The fastest parasitic modes are non-axisymmetric and have the same vertical periodicity as the primary upon which they feed. They tend to have wavevectors that are almost aligned with the velocity or magnetic fields generated by the MRI. As we will detail in a separate paper, the fastest parasitic instabilities can be roughly grouped into Kelvin-Helmholtz and tearing mode instabilities. The first type feed off the sinusoidal velocity field of the MRI and are quenched when the viscosity is increased. The second feed off the MRI currents and are enabled by resistivity.

The values of $\alpha_{\rm sat}$ that result from the rather crude procedure that we followed to find the amplitudes of the MRI fields at saturation are similar, within factors of a few, to the values obtained from numerical simulations in the turbulent regime. Our results suggest, however, that the saturation amplitude of the MRI may not be well determined if the simulation domain limits the available primary and secondary modes. The domains should be large enough vertically to accommodate the fastest primary mode, i.e., $L_z \geq 2\pi/K_{\rm max}(\nu,\eta)$, and should have aspect ratios that allow the fastest parasitic modes, i.e., $L_r, L_\phi \gtrsim 2L_z$ (see §4).

Having gained some insight into the dynamics of primary MRI modes and their parasitic instabilities, it is instructive to review some recent numerical results:

• LL07 carried out a series of shearing box simulations in incompressible MHD with explicit dissipation. For the range of parameters that they explored, $0.1 \lesssim \mathrm{Pm} \lesssim 10$, the stress at saturation decreases with decreasing magnetic Prandtl number. A weak dependence on the Reynolds number cannot be discounted. For several of the runs, the most unstable MRI mode does not fit within the numerical domain, and neither do the fastest parasitic modes. It is worth asking whether the observed trends of $\alpha_{\rm sat}$ with Pm and Re might be biased by these constraints.

• Masada & Sano (2008) explored viscous effects in two-dimensional simulations. In several cases, "saturation" is not achieved since the turbulent stresses are still increasing at the end of the runs. Two different effects might be playing a role in the observed behavior. Axisymmetric parasitic modes grow at only a fraction of the rate of the fastest non-axisymmetric modes. Kelvin-Helmholtz parasites are further slowed by viscosity. Therefore, the MRI field needs to grow to higher amplitudes before the secondary instabilities can compete with the most unstable (available) primary mode.

• Bodo et al. (2008) exposed a dependence of saturation on the aspect ratio of the simulation domain. They found that the saturated stresses decrease when L_r/L_z varies from 1 to 4, and found less significant differences between aspect ratios 4 and 8. We have shown that even in non-ideal MHD, the fastest parasitic modes have horizontal wavelengths roughly twice as large as the vertical wavelength of the dominant primary MRI mode. It is tempting to attribute Bodo et al's (2008) results to the exclusion of parasitic modes at the $1:1$ aspect ratio.

While this Letter was in draft form, we learned of the investigations of Latter et al. (2009, hereafter LLB09), which are similar to our own. A brief comparison of methods and conclusions is in order. Both studies generalize GX94 to resistive MHD and characterize the types and growth rates of the non-ideal parasitic modes. LLB09 neglect viscous effects, which we include, but supplement their analysis with direct numerical simulations. A major conclusion of both studies is that parasitic modes can be limited by the size of the simulation domain. Thus box size may be as important as numerical resolution for the saturation of the MRI.

LLB09 ultimately conclude, however, that parasitic modes are unimportant for two reasons. First, they suggest that parasites should "overtake" the primaries only when the latter reach large non-linear amplitudes, and then the gas behaves compressibly. We have shown that the secondary modes become dynamically important when the MRI magnetic field is of the order of a few times the vertical field. Therefore, we argue that if the initial vertical field is sufficiently weak, then the parasites can erupt before the magnetic pressure approaches the gas pressure, although this regime is expensive to simulate with compressible codes. Second, LLB09 find that in large boxes—where parasitic modes are possible—channel modes emerging from the turbulent regime do not reach large amplitudes; they conclude that something other than parasitic modes must be responsible for their disruption. This may be true, although we suggest another explanation below. While LLB09 speculate about multi-mode interactions, they offer no definite or calculable alternative to parasitic modes. At present, the properties of parasitic modes provide the only analytical guidance, other than the linear MRI dispersion relation, to the choice of dimensions for incompressible or weak-field simulations.

The numerical simulations seem to suggest that the primary modes reach higher amplitudes than predicted in Section 4. Perhaps terms neglected from equations (8) and (9) delay the onset of the secondary instabilities by reducing their growth rates. Alternatively, saturation may occur not when the secondaries achieve the same growth rate as the primary, but when they achieve the same amplitude. The latter occurs later when the MRI develops from a quiet start. Let t_g be the time at which the growth rates match, when the primary has amplitude $B_0(t_g)$. The instantaneous parasitic growth rate $s_{\rm max}(t) \simeq [B_0(t)/B_0(t_g)]\Gamma_{\rm max}$ for $t \geq t_g$. Suppose that the fastest parasite begins with amplitude $\epsilon \ll 1$ relative to the primary at t_g. Then when secondary and primary amplitudes match, at a later time t_a, the primary has grown by a factor $B_0(t_a)/B_0(t_g) \simeq 1 + \ln(1/\epsilon)$. That is, the equal-amplitude criterion predicts a saturation amplitude larger by $\sim \ln(e/\epsilon)$ compared to our previous equal-growth-rate criterion. LLB09 seeded their simulations with small but unspecified noise, which set the initial amplitude of the parasites. If $\epsilon \sim 10^{-4}$ then the overshoot factor $\ln(e/\epsilon) \approx 10$. In the fully turbulent regime, the parasites would start from a larger amplitude, say $\epsilon \sim 0.1$, leading to a smaller overshoot $\ln(e/\epsilon) \sim 3$. Channel modes are then less prominent in the

turbulent state because of this smaller peak amplitude as well as the larger background of other modes. Further numerical investigations should shed light on these issues.

This Letter benefited from trenchant criticism by an anonymous referee. M.E.P. is grateful to Chi-kwan Chan, Peter Goldreich, and Aldo Serenelli for useful discussions and gratefully acknowledges support from the Institute for Advanced Study. This work was supported in part by NSF award PHY-0821899 “Center for Magnetic Self-Organization in Laboratory and Astrophysical Plasmas”.

REFERENCES

Balbus, S. A. & Hawley, J. F. 1991, ApJ, 376, 214
———. 1998, Rev. Mod. Phys., 70, 1
Bodo, G., Mignone, A., Cattaneo, F., Rossi, P., & Ferrari, A. 2008, A&A, 487, 1
Boyd, T. J. M. & Sanderson, J. J. 2003, The Physics of Plasmas (Cambridge: Cambridge University Press)
Chandrasekhar, S 1960, Proc. Nat. Acad. Sci., 46, 253
Fleming, T. P., Stone, J. M., & Hawley, J. F. 2000, ApJ, 530, 464
Fromang, S. & Papaloizou, J. 2007, A&A, 476, 1113
Fromang, S. & Papaloizou, J., Lesur, G.,& Heinemann, T. 2007, A&A, 476, 1123
Goodman, J. & Xu, G. 1994, ApJ, 432, 213
Hawley, J. F., Gammie, C. F., & Balbus, S. A. 1995, ApJ, 440, 742
Knobloch, E. & Julien, K. 2005, Phys. Fluids, 17, 094106
Latter, H. N., Lesaffre, P., & Balbus, S. A. 2009, MNRAS, 394, 715
Lesaffre, P. & Balbus, S. A. 2007, MNRAS, 381, 319
Lesur, G. & Longaretti, P. Y. 2007, MNRAS, 378, 1471
Masada, Y. & Sano, T. 2008, ApJ, 689, 1234
Pessah, M. E. & Chan, C. K. 2008, ApJ, 684, 498
Pessah, M. E., Chan, C. K., & Psaltis, D. 2007, ApJ, 668, L51
Sano, T. 2007, Ap&SS, 307, 191
Sano, T. & Inutsuka, S. I. 2001, ApJ, 561, L179
Sano, T., Inutsuka, S. I., Turner, N. J., & Stone, J. M. 2004, ApJ, 605, 321
Tatsuno T. & Dorland W. 2008, Astron. Nachr., 329, 688
Velikhov, E. P. 1959, JETP, 36, 1398
Vishniac, E. 2009, ApJ, 696, 1021
Umurhan, O. M., Menou, K., & Regev, O. 2007, Phys. Rev. Lett., 98, 034501